3-1990

HD 43246 and HD 127208: Two Unusual F-G + B Binary Systems

Robert C. Dempsey
University of Toledo

Bernard W. Bopp
University of Toledo

Sidney B. Parsons
Space Telescope Science Institute

Francis C. Fekel
Dyer Observatory

Recommended Citation

Robert C. Dempsey et al 1990 PASP 102 312

PUBLICATIONS OF THE ASTRONOMICAL SOCIETY OF THE PACIFIC
102: 312–327, March 1990

HD 43246 AND HD 127208: TWO UNUSUAL F–G + B BINARY SYSTEMS

ROBERT C. DEMPSEY*
Ritter Observatory and Department of Physics and Astronomy, University of Toledo, Toledo, Ohio 43606

SIDNEY B. PARSONS*†
Astronomy Programs, Computer Sciences Corporation, Space Telescope Science Institute
3700 San Martin Drive, Baltimore, Maryland 21218

BERNARD W. BOPP*†
Ritter Observatory and Department of Physics and Astronomy, University of Toledo, Toledo, Ohio 43606

AND

FRANCIS C. FEKEL*
Dyer Observatory, Vanderbilt University, Nashville, Tennessee 37235

Received 1989 September 13, revised 1989 December 4

ABSTRACT

New optical spectroscopic observations along with ultraviolet IUE observations have been obtained for the two interacting F or G III + B V binaries: HD 43246 and HD 127208. Photometric observations indicate random changes superimposed on regular ellipsoidal light variations, the latter probably the result of tidal distortion of the giant primaries. Mass transfer and loss is apparent in inverted mass ratios derived from orbital analysis, strong wind features present in the spectra, and the presence of circumsystem shells. Regular and irregular changes in the spectral features are discussed in this context.

Key words: stars: emission-line–stars: radial velocities–stars: binaries

1. Introduction

During the early emission-line surveys of the Harvard College Observatories, begun by Pickering in 1886, several F stars with bright hydrogen emission were detected. Emission-line stars among spectral classes A through K are exceedingly rare. Merrill (1942) classified many of these as cFe. Bidelman (1954) later disentangled their spectra, identifying them as a composite of a Be star and an F star of Type II or III.

The existence of Be stars in binary systems poses many questions. Hydrogen emission in Be stars, along with emission from other species such as Mg II and Fe II, is probably formed either in an extended atmospheric region of the star or in a disk or ring of material surrounding the star (Underhill 1982 and references therin; Hanuschik 1986). That these stars also appear to be rapid rotators, as indicated by their broad He I absorption lines (Slettebak 1976), suggests a connection between the Be phenomenon and v_{eq}. Thus, we would not expect to find Be stars in short-period binaries, since tidal interactions would quickly slow the rapid rotation of the Be star. In fact, there does appear to be an absence of such short-period systems (Batten, Fletcher, and Mann 1978; Abt and Levy 1978). Additionally, Abt and Cardona (1984) confirmed the nearly complete absence of Be stars with periods of a month or less, although such periods occur quite frequently among B stars. For periods greater than 35 days Abt and Cardona claim there is apparently no discernible difference in binary frequency between B and Be stars. These results must be viewed with caution due to the inherent difficulty in detecting small-amplitude binary motion in Be stars since the spectral lines are very broad and are frequently blended with emission or shell absorption. For example, two stars (HR 2142 and HR 7084) which Abt and Cardona claimed to be single are actually interacting binaries (Peters 1981).

The frequency of F or G giants or supergiants in binary systems is also difficult to determine. Main-sequence stars are often found to be binaries, with estimates of the rate of duplicity ranging from about 40% to 100%, but usually believed to be about 84% (Abt 1983). Along the main sequence, numerous systems are found with peri-

*Visiting Astronomer, Kitt Peak National Observatory, National Optical Astronomy Observatories, operated by the Association of Universities for Research in Astronomy, Inc., under contract with the National Science Foundation.

†Guest Observer with the International Ultraviolet Explorer Satellite.

ods of a few days. Abt (1983) reported that normal giants are nearly absent in binary systems with periods less than 10 days and deficient in systems with periods less than 100 days. For longer periods the rate of duplicity appears to be the same as for the main sequence. The percentage of supergiants in binary systems, though not well-known, is lower than that of stars among the main sequence. It is also found that binary systems having a supergiant component tend to have very long periods. Burki and Mayor (1983) found a total rate of binaries among F–M supergiants to be 31% to 38% with no significant dependence on spectral type. Some surveys have been done on the related class of Cepheids, which are pulsating F and G supergiants. In order for the Cepheid primary to cross the instability strip at least two times, the binary must have a minimum period of about 200 days (Lloyd Evans 1968). Estimates of duplicity among Cepheids range from 25% to 35% (Madore 1977; Madore and Fernie 1980; Russo 1982) but might be as high as 40% (Gieren 1982). Therefore, a binary system consisting of a supergiant with a period of less than 200 days would be rare.

In light of these circumstances, the F + Be systems with periods of less than 100 days warrant further investigation. The research presented here is part of an ongoing study of binary systems containing a Be star with an evolved F-, G-, or K-type star. Currently, six such objects are being monitored by us. Results for the simplest of these, HR 2577 (MWC 827, K2 II + B3 IVe), were presented as a benchmark for the more complex systems since it appears to be a widely separated and noninteracting system (Dempsey, Parsons, and Bopp 1988). In the other systems the emission phenomenon appears to be a direct result of interaction between the components, and the use of Be for the classification of the hot component in the classical sense becomes questionable. Nonetheless, such short-period binaries present excellent opportunities for understanding binary interaction as well as providing further insight into the binary model for Be stars proposed by Kriz and Harmanec (1975). These interacting binary systems divide into two categories. The first group includes HD 37453 (F5 II + Be, Bidelman 1954) and HD 207739 (F8 II +Bvp, Parsons and Bopp 1986) having periods of 66 and 141 days, respectively. Results for HD 207739 are discussed in Griffin *et al.* (1990) while those for HD 37453 will be presented in a future paper. In the second group, described here, are HD 43246 (F5 III + B8 V, Petrie 1948) and HD 127208 (F III + B V). Characteristics that distinguish stars in the first group include stronger Hα emission, the presence of [N II] emission and He I λ5876 absorption, and larger mass functions ($\sim$ 2–5 $\mathfrak{M}_\odot$). We present new photometric and spectroscopic observations for HD 43246 and HD 127208 that show these systems to be short-period binaries ($P <$ one month) with the primaries being tidally distorted and apparently undergoing mass transfer. In particular, observations of the Na I D region indicate the presence of circumstellar material. Additionally, we discuss Hα and International Ultraviolet Explorer Satellite (IUE) observations of the systems.

2. Observations

Optical spectroscopic data for HD 43246 and HD 127208 were obtained from three observatories over an interval of about seven years, beginning in 1979. Table 1 lists the telescopes, dispersions, resolutions, and detectors used. CF designates the coudé feed telescope at Kitt Peak National Observatory (KPNO) where TI and RCA CCD detectors and IIa-O photographic plates were used primarily with camera 5. RO refers to the Ritter 1-meter telescope at the University of Toledo, where an intensified Reticon was used with a fiber-coupled echelle spectrograph (Bopp, Noah, and Jones 1985). Finally, MC designates the McDonald Observatory 2.7-meter telescope and a Reticon detector (Fekel 1988). Photographic plates recorded the Hα wavelength region and used a Carnegie image tube. Estimates of signal-to-noise ratio (*S/N*) for the CCD data typically range between 50:1 and 100:1; the intensified Reticon spectra typically have a *S/N* between 10:1 and 30:1. The CCD and Reticon data reductions were carried out with standard methods. Bias levels were subtracted from each stellar observation which was then divided by flat-field lamp scans to correct for pixel-to-pixel variations in sensitivity. For observations of each night one or more comparison spectra of a thorium-argon hollow-cathode or neon lamp were obtained for wavelength calibration.

UBV photometric observations of the systems were obtained by one of us (B.W.B.) during the interval July 1982 through May 1985 at KPNO with the No. 2 0.9-meter telescope. These measurements were made in an attempt to detect any light variations, especially those which could be linked to spectroscopic variations. Bopp *et al.* (1984) describe the method of photometric data-acquisition and reduction routines. The *UBV* measures

TABLE 1

Telescope Information

Telescope	Detector	Dispersion (Å/mm)	Resolution (Å)
CF1	TI3	7.6	0.23
CF2	TI3	14.8	0.89
CF3	RCA	14.8	0.89
CF4	RCA	7.6	0.23
CF5	PLATE	15.0	0.60
CF6	RCA	4.2	0.30
CF7	TI3	7.0	0.19
RO	RETICON	2.5	0.35
MC	RETICON	4.4	0.36

are shown in Tables 2 and 3.

3. Radial Velocities and Orbits

In the visible portion of the spectrum both systems are seen as single-lined spectroscopic binaries where the absorption lines arise from the cooler (primary) component. Radial-velocity measurements of the primaries were made with cross-correlation techniques or by manually measuring individual line shifts ("line by line"). The errors for the cross-correlation technique are estimated to be about 1 km s^{-1} (Bopp and Meredith 1986). Tables 4 and 5 list the radial-velocity measures and, where appropriate, the standard deviation of the mean for line-by-line measurements or the radial-velocity standard star used in the cross correlation. Additionally, Table 4 includes values with either the technique described by Fekel, Bopp, and Lacy (1978) or Willmarth and Abt (1985) and are designated as FBL or W in Table 4, respectively.

TABLE 2

Photometric Data: HD 43246

HJD 2,440,000+	V	B-V	U-B
5274.9820	7.418	0.408	-0.158
5275.9780	7.418	0.422	-0.162
5276.8840	7.427	0.413	-0.156
5276.9420	7.426	0.408	-0.144
5277.8940	7.416	0.415	-0.156
5278.9440	7.407	0.417	-0.157
5279.8760	7.385	0.422	-0.141
5280.0010	7.383	0.422	-0.142
5328.8640	7.335	0.432	-0.137
5330.8070	7.379	0.418	-0.148
5330.8460	7.372	0.421	-0.149
5330.8780	7.380	0.420	-0.154
5424.6330	7.386	0.416	-0.142
5425.6550	7.410	0.418	-0.148
5723.7500	7.369	0.412	-0.140
5724.7000	7.374	0.408	-0.153
5725.8000	7.388	0.407	-0.157
5726.7000	7.424	0.398	-0.180
5778.6832	7.380	0.414	-0.130
5779.7483	7.361	0.425	-0.117
6129.6651	7.356	0.411	-0.158
6129.6963	7.359	0.415	-0.155
6129.7470	7.376	0.410	-0.145
6185.6286	7.371	0.404	-0.126
6186.6237	7.342	0.414	-0.132
MEAN	7.386	0.415	-0.147
±	0.005	0.001	0.003

Comparison: SAO 078186
V = 7.735 ± 0.004
(B-V) = -0.192 ± 0.001
(U-B) = -0.138 ± 0.003

Once a large-enough base of radial velocities was obtained, three steps were followed to calculate the orbital elements. First, a simple period-finding program was used to get approximate periods. Approximate orbital elements were then found with the program of Wolf, Horak, and Storer (1967). Finally, a more sophisticated program, SBIN2 (Barker, Evans, and Laing 1967), used an iterative approach with the preliminary values of the elements to generate the final values by least-squares fitting. The program SBIN2 also allows one to choose a weighting factor for each radial velocity. Values obtained from individual lines were given half-weight while all others were given full weight due to their higher precision. The values of the final orbital elements are given in Tables 6 and 7. The radial velocities and the derived orbits are shown in Figures 1 and 2. Values of $O-C$ (observed minus calculated) for the radial velocities are listed in Tables 4 and 5. For HD 127208 the eccentricity was found to be within two standard deviations of zero and was therefore taken to be zero. Phases for both systems are computed from conjunction with the F star closest to the observer. Mass functions for both systems were found to be greater than unity; therefore, it is likely that the evolved primaries are the lower mass components (see below), indicating that substantial mass transfer has taken place.

Petrie (1948) also determined orbital elements for HD 43246 from 34 DAO spectra and five earlier Mount

TABLE 3

Photometric Data: HD 127208

HJD 2,440,000+	V	B-V	U-B
5778.9117	6.964	0.238	-0.319
5779.9118	6.954	0.214	-0.362
5779.9861	6.956	0.220	-0.370
5837.7195	6.973	0.195	-0.323
5837.7535	6.977	0.205	-0.341
5837.7896	6.959	0.218	-0.343
6185.7887	6.945	0.242	-0.340
6223.7451	6.950	0.225	-0.355
6225.7159	7.003	0.209	-0.441
MEAN	6.945	0.218	-0.355
±	0.006	0.005	0.012

Comparison: SAO 182654
V = 7.248 ± 0.005
(B-V) = 0.984 ± 0.003
(U-B) = 0.768 ± 0.013

TABLE 4

Radial velocities for HD 43246

HJD 2,440,000+	PHASE	Rv km/s	ERROR/STD km/s /	O - C km/s	SOURCE
3965.6550	0.428	37.8	1.1	-0.7	CF5
4357.6255	0.341	75.0	Beta Gem	2.8	MC, FBL
4507.0140	0.787	-69.0	1.5	-1.9	CF5
4508.0030	0.830	-57.0	1.4	2.4	CF5
4509.9800	0.915	-31.5	2.2	-0.7	CF5
4511.9440	0.000	6.8	1.0	-2.0	CF5
4512.9710	0.044	30.6	0.9	0.1	CF5
4627.7164	0.996	8.4	Beta Gem	1.8	MC, FBL
5231.9930	0.070	40.1	1.4	-2.1	CF3
5358.7264	0.538	-14.5	10 Tau	0.0	CF6, FBL
5360.8305	0.629	-51.1	Beta Gem	-0.3	CF6, FBL
5361.7860	0.670	-63.7	10 Tau	-2.0	CF6, FBL
5420.6155	0.208	87.5	1.8	2.5	CF3
5422.6415	0.296	84.2	2.0	1.2	CF3
5425.7131	0.428	35.7	3.5	-2.7	CF3
5599.9949	0.948	-15.5	0.6	0.6	CF1
5602.9847	0.077	46.9	0.8	1.1	CF4
5719.8799	0.121	64.3	Beta Gem	0.8	CF1, W
5720.8365	0.163	77.2	Beta Gem	0.8	CF1, W
5721.7647	0.203	81.2	Beta Gem	-3.1	CF1, W
5788.7033	0.091	48.0	0.7	-3.6	CF4
5790.6287	0.174	78.7	Beta Gem	-0.4	CF4
5792.6454	0.261	87.4	61 UMa	0.6	CF4
5793.6459	0.304	81.0	61 UMa	-0.4	CF4
5794.6980	0.349	66.2	1.9	-3.6	CF1
5811.6343	0.080	47.9	Beta Gem	0.8	CF1, W
5812.6383	0.124	64.6	Beta Gem	0.2	CF1, W
5813.6490	0.168	77.1	Beta Vir	-0.5	CF1, W
5987.9152	0.687	-66.4	Alpha Ari	-1.5	CF1
6023.8842	0.239	88.6	10 Tau	1.4	CF1
6126.6418	0.673	-57.8	61 UMa	4.5	CF2
6137.7077	0.150	72.2	61 UMa	-0.8	CF3
6338.9377	0.833	-60.1	Alpha Ari	-1.4	CF1
6340.9267	0.919	-29.2	Alpha Ari	0.0	CF1
6341.9861	0.965	-7.9	Alpha Ari	0.6	CF1
6391.0311	0.081	47.8	Beta Gem	0.5	CF1, FBL
7097.0249	0.544	-16.4	10 Tau	0.9	CF1, W
7151.9927	0.916	-30.9	Beta Gem	-0.3	CF7, W
7152.9675	0.958	-11.0	Beta Gem	0.7	CF7, W

The columns are as follows: Heliocentric Julian date of observation, orbital phase, radial velocity of the F star, either the standard deviation of the mean for line-by-line or the radial velocity standard star used in the cross-correlation, the observed velocity minus calculated (O-C), and finally telescope configuration. FBL and W in the last column designate measuring technique if it differs from "line-by-line" or Bopp and Meredith (1986). The velocities for the standards (taken from GCRV) are as follows: +3.3, +27.9, -5.4, +5.0 and -14.3 km/s for β Gem, 10 Tau, 61 UMa, β Vir and α Ari, respectively.

Wilson observations (Christie and Wilson 1938). We attempted to combine the older data with our radial velocities in an effort to improve the orbital solution. Unfortunately, this proved unsuccessful. While Petrie's *period* for the system agrees extremely well with ours, there are notable differences in other orbital elements. Petrie's

TABLE 5

Radial Velocities for HD 127208

HJD 2,440,000+	PHASE	Rv km/s	Error/Std km/s /	O - C km/s	SOURCE
5420.9577	0.204	61.4	2.8	2.6	CF3
5420.9619	0.204	61.8	2.6	3.0	CF3
5422.9026	0.283	60.1	1.8	-0.4	CF3
5423.9457	0.325	56.1	2.6	3.1	CF3
5787.8675	0.110	27.8	1.5	-3.9	CF4
5788.8837	0.151	40.3	1.3	-6.3	CF4
5790.8864	0.232	61.9	2.2	0.1	CF4
5792.8929	0.314	52.8	1.0	-2.7	CF4
5793.8756	0.354	45.7	2.2	0.8	CF4
5794.9104	0.396	30.0	1.5	0.7	CF1
5872.7375	0.558	-49.9	1.5	1.9	CF1
5872.7424	0.558	-54.6	1.8	-2.7	CF1
5872.7608	0.559	-56.2	1.5	-4.0	CF1
6125.9698	0.846	-90.0	61 UMa	1.3	CF2
6126.9615	0.886	-77.5	61 Uma	-0.4	CF2
6128.9706	0.968	-39.2	61 UMa	-0.3	CF2
6129.8977	0.005	-17.1	61 Uma	2.0	CF2
6137.9582	0.333	53.1	61 Uma	1.9	CF4
6138.9361	0.372	41.3	61 Uma	2.7	CF4
6937.8222	0.828	-94.5	5 Ser	1.6	CF2
6938.7607	0.866	-81.6	5 Ser	3.0	CF2
6939.8120	0.909	-66.9	5 Ser	0.6	CF2
6940.7634	0.947	-49.3	Beta Oph	-0.1	CF2
6943.7219	0.068	10.5	5 Ser	-2.3	CF2
6943.8056	0.071	10.9	Kappa Her	-3.5	CF2
6944.7306	0.109	30.0	5 Ser	-1.2	CF2
6944.8782	0.115	32.6	Kappa Her	-1.0	CF2
6945.7064	0.148	46.6	Alpha Boo	1.0	CF2

The columns are as follows: Heliocentric Julian date of observation, orbital phase, radial velocity of the G star, either the standard deviation of the mean for line-by-line or the radial velocity standard star used in the cross-correlation, the observed velocity minus calculated (O-C), and finally telescope configuration. The radial velocities for the standards were as follows: +53.5, -12.0, -9.5 and -5.3 km/s for 5 Ser, β Oph, κ Her and α Boo, respectively.

value for K, the semiamplitude of the primary, is smaller by about 11 km s^{-1} and his systemic velocity (γ) is also smaller by about 6 km s^{-1}! The possibility of a systematic shift was investigated but this does not seem to be the case here since this does not explain the smaller amplitude. Analysis of Petrie's data (for the F star) with our programs confirmed his solution. It is likely that the discrepancy is due to measuring differences or errors. Another possibility is the presence of an undetected third component with a period that is much longer than the binary period (probably on the order of years). This would explain both the change in γ and K, the latter due to nodal precession caused by the presence of the third star. We derive a value of $\Delta K/K \sim 0.15$. This is more than twice as large as most values found by Mayor and Mazeh (1987) for systems they concluded were probably triple. Since the γ velocity apparently remained constant during each set of observations, the period of the third star would have to be greater than the two observing periods, or about 12 years. While this does not prove the existence of a third body the possibility should be investigated further. Since the rate of triple systems among binary stars may be between one-third (Batten 1973) to one-half (Mayor and Mazeh 1987) this hypothesis is not unreasonable.

We note that Petrie's orbital solution included measures of a narrow and weak Ca II K line which he attributed to the hotter (secondary) component. The K-line observations showed a large scatter, but Petrie derived an orbital solution using these measures that indicated the hot component was the more massive but was also underluminous. However, our blue spectrograms (source = CF5 in Table 4), which have better resolution and are more heavily exposed than Petrie's prism spectrograms, show the K line as very narrow ($v \sin i < 10$ km s^{-1}) and clearly *not* photospheric in origin. The line shows a constant radial velocity of $+10.9 \pm 0.7$ km s^{-1} and is probably produced in a circumstellar shell (see below). We conclude that Petrie's observations of a variable K-line velocity are spurious and that there is no evidence that the hotter component in HD 43246 is subluminous.

TABLE 6

Parameters for HD 43246

P (days)	23.1755	± 0.0006
T (2,440,000+) HJD	3978.905	± 1.34
γ (km/s)	7.5	± 0.4
K (km/s)	78.5	± 0.5
e	0.016	± 0.006
ω (degrees)	270	± 20
f(m) (M_o)	1.16	± 0.02
a sin i (10^6 km)	25.0	± 0.4
v sin i	23	
R (10^6 km)	10	
a (10^6 km)	33	
i (degrees)	48	
R_L (10^6 km)	26	

TABLE 7

Parameters for HD 127208

P (days)	24.615	± 0.002
T_o (2,440,000+) HJD	6942.06	± 2.78
γ (km/s)	-22.9	± 0.8
K (km/s)	84.1	± 1.0
e (assumed)	0.0	
f(m) (M_o)	1.52	± 0.06
asin i (10^6km)	28.5	± 0.3
v sin i	19	
R (10^6 km)	12	
a (10^6 km)	38	
i (degrees)	56	
R_L (10^6 km)	107	

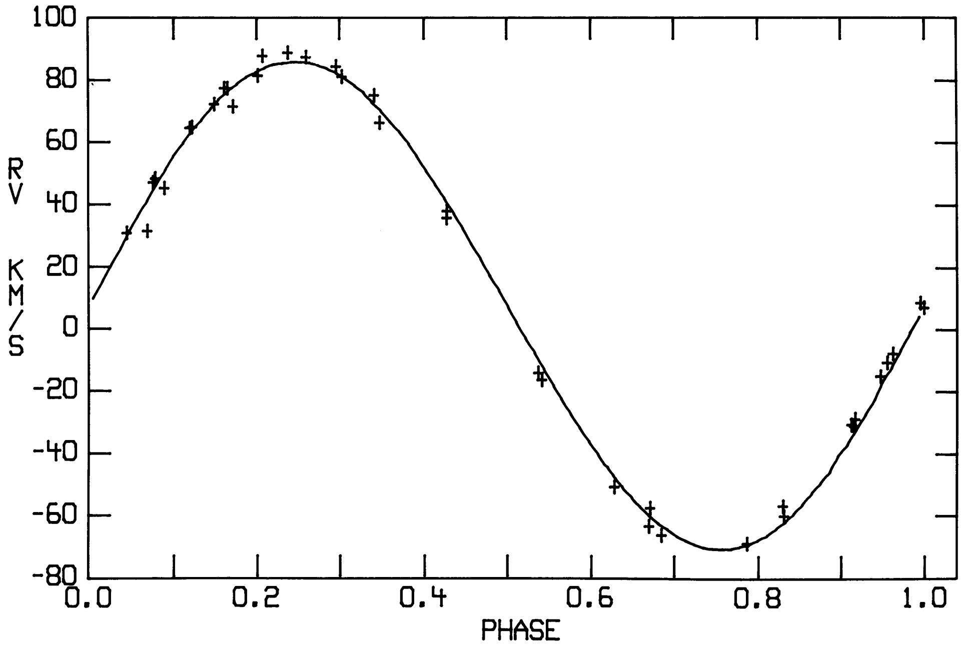

FIG. 1–New orbit for HD 43246. Pluses indicate observed radial velocities from Table 4 while the solid line depicts the theoretical curve derived from the orbital elements listed in Table 6.

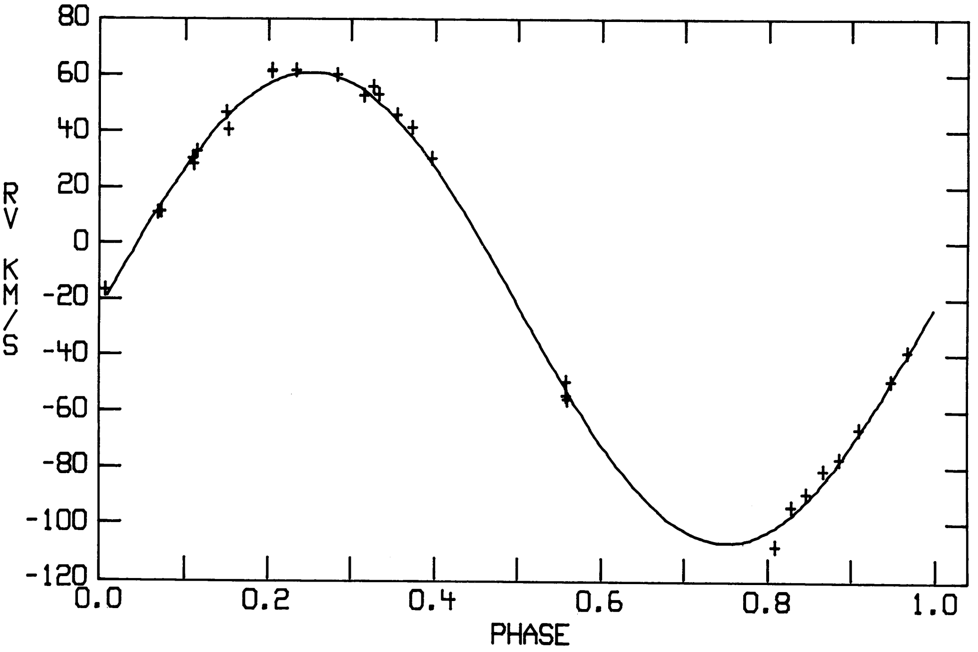

FIG. 2–Orbit for HD 127208 with pluses indicating observed radial velocities from Table 5 and the solid line showing the theoretical curve derived from the orbital elements in Table 7.

4. Photometry

Once the orbital periods of the systems had been firmly established, the photometry was plotted as a function of phase. The results for HD 43246 are shown in Figure 3. While the data are incomplete in phase coverage, both systems clearly display considerable variations (Tables 2 and 3) and, at least for HD 43246, a double sine wave pattern (Fig. 3). It is postulated that the double sine wave is produced by ellipsoidal variations of the stars. From the equations of Morris (1985) for noneclipsing systems with ellipsoidal light variations, estimates of stellar radii, the mean separation of the stars, and the orbital inclination were obtained. Limb-darkening coefficients were taken

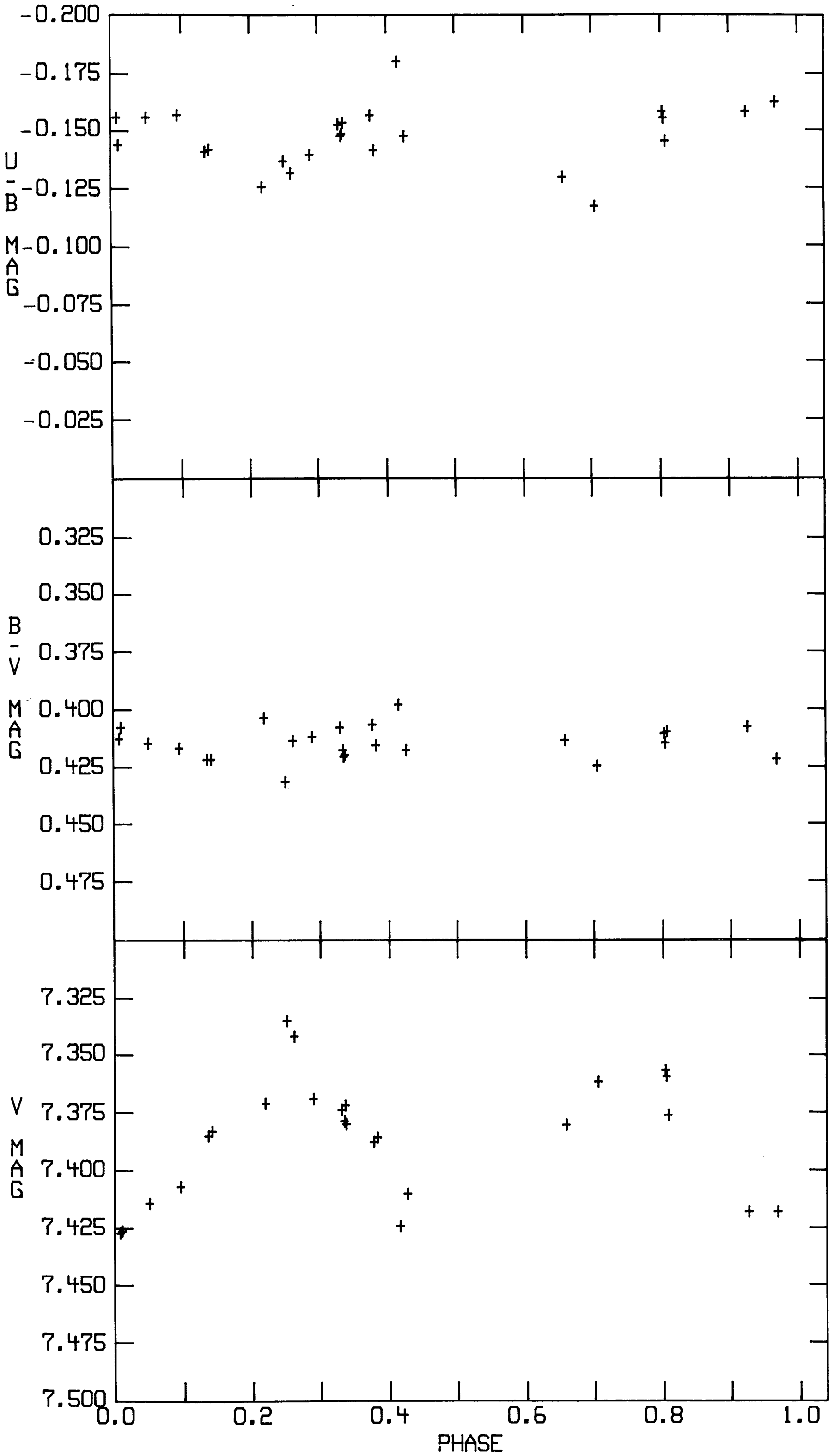

FIG. 3–Light curves for HD 43246 obtained during the interval October 1982 to May 1985. Phases are from Table 6. The variations in V are in the form of a double sine wave, indicating ellipsoidal variability.

from Grygar, Cooper, and Jurkevich (1972) and approximate values for $v \sin i$ were obtained by measuring the width of several narrow lines. The results are also listed in Tables 6 and 7. Values of 14 and 17 $R_\odot$ were derived for

HD 43246 and HD 127208, respectively. These radii are greater than the average values of about 4 $R_\odot$ for F5 III stars and 10 $R_\odot$ for G5 III stars (Allen 1976). These radii are an appreciable fraction of their Roche-lobe radii (R_L), calculated with the equation of Pacynski (1971), also listed in Tables 6 and 7. While the ellipsoidal nature of HD 127208 cannot be firmly established with the current incomplete light curve, its similarity to the other F + Be systems under study suggests this indeed is the case. The above analysis is not seriously affected by the incompleteness provided the amplitude of the variation is representative. IUE observations have found small mid-UV excesses which may indicate accretion disks in these systems (see below). While this could affect the above analysis the impact appears to be minor since good agreement was found between the V, $(B-V)$, and $(U-B)$ light curves and since, except for the mid-UV excess, the UV spectra of the B stars appear essentially normal.

Adopting a mass of 4.3 $\mathfrak{M}_\odot$ for the secondary of HD 43246 (Allen 1976, using the IUE spectral type below) and using the value obtained for sin i in conjunction with the mass function calculated in Section 3, we derive a mass for the F primary of about 1 $\mathfrak{M}_\odot$. A similar, but more uncertain, result follows for HD 127208. Therefore, in both systems the evolved primary is the lower mass component indicating that mass transfer has taken place.

In addition to ellipsoidal behavior there are also unequal maxima and minima in V. The light curves also exhibit light fluctuations or "flickering", especially in HD 127208 where the amplitude of variation in $(U-B)$ is greater than that of HD 43246. In both systems the $(B-V)$ light curves exhibit the least variation. Since mass transfer has taken place in the past and may well be occurring currently, it is possible that the flickering in the light curves arises due to other matter in the system such as a stellar wind, a stream, or an accretion disk.

5. Spectroscopic Observations

5.1 *Optical*

Hα is observed in emission in both HD 43246 and HD 127208, typically with equivalent widths of about 4 Å. Several spectra of each system are displayed in Figures 4 and 5. The equivalent width (W_λ) varies considerably in both systems. Errors for W_λ are estimated to be 10% due primarily to uncertainties in continuum placement. Variations of 10%–30% argue convincingly that the variations are real. Observations spread over several days indicated that W_λ remains constant (variations less than or equal to 10%) over short intervals of time. There was no indication of any change between two spectra taken on the same night.

All observations of HD 127208 and those for the first half of the orbit for HD 43246 display a strong absorption feature blueward of the main emission; this is indicated by the short vertical lines in Figures 4 and 5. For HD 43246 the absorption is not present from phase 0.0 to 0.5 and

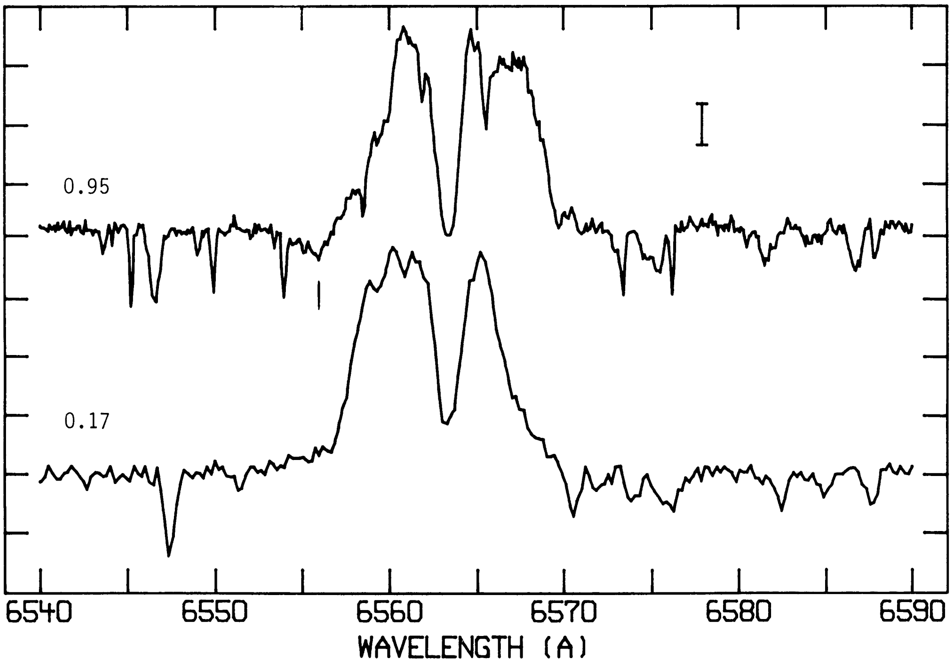

FIG. 4–Hα composite for HD 43246 showing profile variations, especially the change in the shallow absorption on the blueward side of the main emission (top spectrum) and the shift in the central reversal. The spectra are from the bottom to top: JD2445790.6 and JD2445600.0 with phases 0.17 and 0.95, respectively. The spectra have been normalized and shifted arbitrarily in the vertical direction for clarity and shifted horizontally to be approximately in the rest frame of the Sun. The bar indicates 10% of the continuum level and the numbers to the left indicate the phase of the observation. The short line in the top spectrum marks the wind absorption discussed in the text. The many sharp lines in the top spectrum are telluric water-vapor lines. The Y axis is relative intensity.

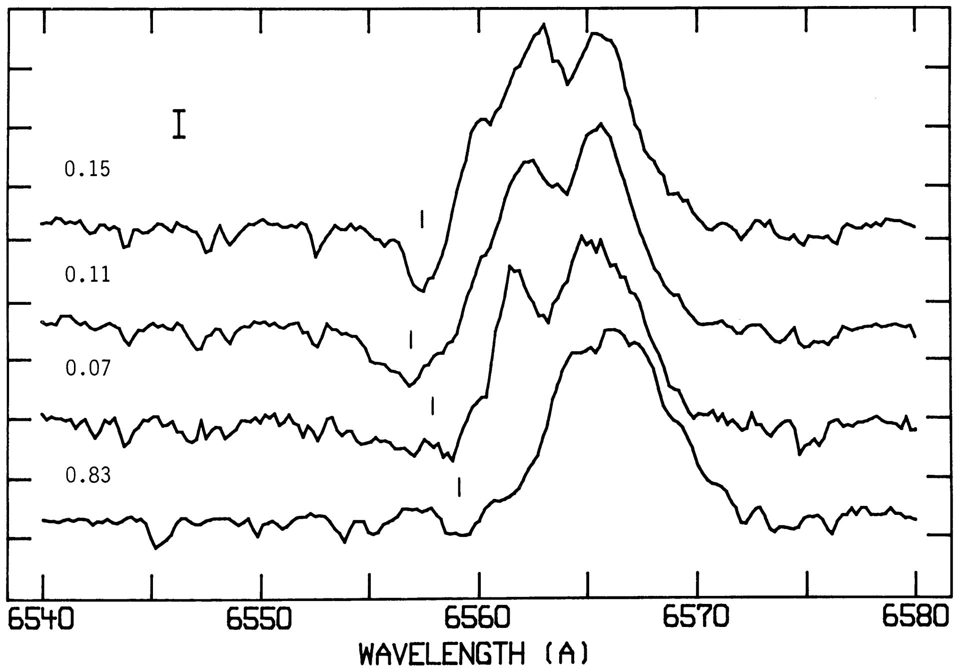

FIG. 5–Hα composite for HD 127208 showing profile variations described in text. The spectra are from bottom to top: JD2446937.8, JD2446943.7, JD2446944.7, and JD2446945.7 at phases 0.83, 0.07, 0.11, and 0.15, respectively. The spectra have been treated as in Figure 5. The absorption produced by the wind from the B star is marked as in Figure 4. Phases are indicated by the numbers on the left. The y axis is relative intensity.

there may be a slight rise above the continuum. The feature then appears around phase 0.5 and the central velocity shifts from about -420 km s^{-1} to -340 km s^{-1}. Though the scatter is high due to measurement difficulties such as asymmetry in the feature, telluric water contamination, and poor phase coverage, the velocity of this feature in both systems changes in the opposite sense of the radial-velocity curve. Therefore, the Hα emission is likely due to a wind at or near the B star. A similar result is obtained for HD 127208, but with considerably more scatter, by measuring the central velocity of the Hα emission. The center of Hα was defined to be the midpoint at the base of the emission. The residual intensity of the absorption feature in HD 127208 appears to undergo phase-related changes, reaching a maximum depth around phase 0.25. For all spectra of HD 43246 and for many of HD 127208 a central reversal in the emission is present. Though measuring the velocity of this feature is hampered as well there does appear to be a definite trend to follow the cool component though with a lower amplitude. These variations can be seen in Figures 4 and 5. Numerous other smaller absorption features are frequently observed in addition to the main central reversal. Though phase coverage is not adequate and contamination by telluric features is high in some spectra, observations spread over several days indicate that these features follow the orbital motion of the primary as well.

Further evidence that the changes seen in Hα are tied to orbital motion comes from comparing spectra taken several years apart. For example, two spectra of HD 127208 taken three years apart (the later of which is the second spectrum from the top in Fig. 5) have identical profiles with equivalent widths that are within 5% of each other. Plotting W_λ versus phase suggests the possibility of phase dependence but scatter is high. There are quite likely erratic, stochastic variations superimposed on regular, orbit-related changes. In general the behavior of the Hα emission is rooted in orbital behavior. Much of the variation is due to the shifting central reversal that arises from the cool component of both systems. At certain phases for HD 127208 the central reversal is Doppler shifted to its most negative velocity when the wind absorption reaches its greatest redshift. The two features meet producing a very broad depression on the blueward side of the emission. As the stars revolve, the reversal follows the G star, overlapping the emission, and creating an "eaten-away" appearance that eventually produces the fully developed central reversal which continues to shift across the emission.

The case is slightly different for HD 43246 since the broad "wind" absorption is not always present. If in this case the deep absorption arises from the F star, either as a wind or more concentrated mass flow such as a stream, it is possible that the feature gets shifted to overlap the emission from the B star and is thus filled in and lost. The fact that the wind feature appears to follow the B star is a problem with either interpretation, but since there are only five such observations with high scatter, it is possible that this apparent motion may be erroneous. Additionally, the central reversal is never blueshifted enough to overlap the wind feature as in HD 127208 but instead always splits the emission.

Small fluctuations observed at Hα and in the light curves may well arise from turbulent motions in a disk or ring surrounding the B star. Weaker absorption features in Hα apparently arise at or near the F or G star, perhaps in a mass stream.

Scans of the Na D region display double Na D absorption (Fig. 6). The Na D lines consist of broad, shallow absorption lines, which will be designated "photosphere" since they apparently arise from the photosphere of the cool component, along with narrow, deep absorption lines. The narrow components, with velocities that are constant, though shifted about $+10$ km s^{-1} from γ, are likely the result of a circumstellar shell around the systems. We rule out the possibility that the narrow components are interstellar in origin for two reasons. First, there is considerable variability in the equivalent widths and core depths of the components (over 30% in 2 days for HD 43246). This suggests the line-forming region for these components lies near the interacting systems. Furthermore, we derive small values for $E(B-V)$ (see below) for the systems, implying that they are not very distant and therefore their spectra are not likely to display strong interstellar absorption lines. Velocities of the broad, shallow components vary in phase with the radial-velocity curve and must therefore arise from the primary.

5.2 *IUE Low-Resolution Spectroscopy*

Details of the IUE satellite observations of HD 43246 and HD 127208 are presented in Tables 8 and 9. The first column gives the IUE camera (Long/Short Wavelength Prime/Redundant), sequence number, and dispersion (high or low). Exposure times are given in minutes:seconds in the second column. The third and fourth columns give the calendar and Heliocentric Julian Date of midexposure. The phase in the fifth column is with respect to the conjunction when the cool component is closer to the Earth; these epochs are 2443978.91 and 2446942.06, respectively, for HD 43246 and HD 127208. The last three columns give selected binned fluxes, as described in Section 5.3, centered at the wavelengths indicated.

The far-UV (SWP camera) spectra of HD 43246 and HD 127208 have been compared to IUE spectra of standard stars (Wu *et al.* 1983). Both binary systems have peculiar spectra due to ionized plasma features (below), but both may be classified as B8–9 III–Vp. They are matched most closely by the B9 IV star α Delphini = HD 196867 (Fig. 7). The spectra of the program stars at different epochs have been coadded, after compensation for any significant velocity or registration differences. However, three of the nine observations of HD 43246 were found to differ significantly from the mean spectrum and were deleted from the final coaddition.

Differences between the coadded spectra and the α Del spectrum are also displayed in Figure 7. These difference spectra show absorption from Si IV and C IV, and probable emission at C II 1335. The three maverick spectra of HD 43246 (images 24257, 27059, and 32164) have more pronounced features at these wavelengths: deeper

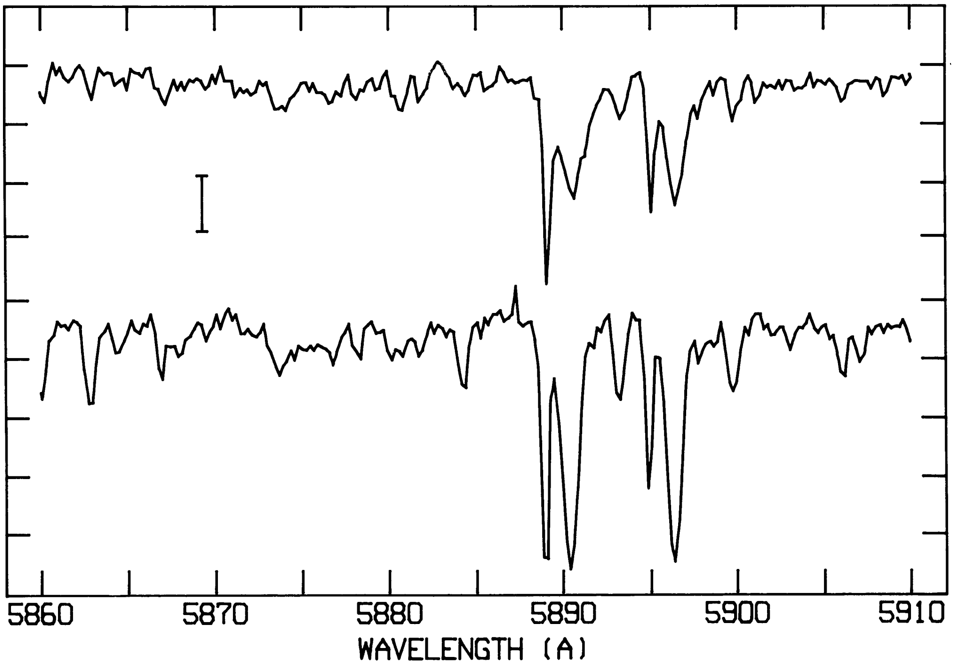

FIG. 6–Normalized spectra of the Na I D region of HD 43246 (bottom) and HD 127208 (top) showing the narrow circumstellar absorption to the left (in both spectra) of the broader photospheric lines. The bar indicates 10% of the continuum. A small noise spike appears to the left of the lines in the bottom spectrum. The observations are from JD2445792.6 (bottom) and JD2445792.9 (top). The *Y* axis is relative intensity.

TABLE 8

IUE observation details for HD 43246 (phase = 43978.905+23.175)

FRAME,DISP	EXP. TIME	YR/MO/DAY	MID-EXP. JD-2440000	PHASE	FLUX MAGNITUDE		
LWR/LWP					(2150)	(2550)	(2950)
LWR 9655L	1:15	81/01/07.1	4611.626	0.30	7.34	7.43	7.48
LWR 9656H	45:	81/01/07.2	4611.68	0.30	7.49:	7.44:	7.46:
LWR16775H	35:	83/09/12.4	5589.44	0.49	7.44:	7.46:	7.49:
LWR16834H	25:	83/09/21.2	5598.66	0.89	7.42:	7.56:	7.44:
LWR16853L	1:06	83/09/23.4	5600.912	0.99	7.44	7.56	7.54
LWP 4497H	25:	84/10/04.2	5977.73	0.25	7.34:	7.38:	7.39:
LWP 4605L	1:06	84/10/22.2	5995.738	0.02	7.52	7.45	7.52:
LWP 4606H	35:	84/10/22.3	5995.78	0.03	7.21::	7.38:	7.42:
LWP 4744H	37:	84/11/07.3	6011.77	0.72	7.32:	7.37:	7.36:
LWP 5250H	35:	85/01/23.1	6088.56	0.03	7.22:	7.41:	7.40:
LWP 7060H	30:	85/11/09.4	6378.88	0.56	7.43::	7.55:	7.53:
LWP11956H	45:	87/10/26.3	7094.795	0.45	7.28:	7.46:	7.44:
SWP					(1450)	(1650)	(1850)
SWP10988L	1:20	81/01/07.1	4611.624	0.30	6.79	7.04	7.19
SWP21026L	3X 1:20	83/09/12.5	5589.955	0.52	6.80	7.04	7.19
SWP21115L	3X 1:20	83/09/21.1	5598.641	0.89	6.82	7.14	7.24
SWP21138L	3X 1:30	83/09/23.4	5600.903	0.99	6.82	7.13	7.27
SWP24109L	1:40	84/10/04.2	5977.745	0.25	6.80	7.10	7.23
SWP24257L	1:50	84/10/22.2	5995.742	0.02	6.81	7.14	7.23
SWP24951L	2:00	85/01/23.0	6088.544	0.03	6.76	7.11	7.23
SWP27059L	2:20	85/11/09.4	6378.897	0.56	6.78	7.12	7.23
SWP32164L	1:54	87/10/26.3	7094.814	0.45	6.77	7.11	7.23

TABLE 9

IUE observation details for HD 127208 (phase=46942.06+24.615E)

FRAME,DISP	EXP. TIME	YR/MO/DAY	MID-EXP. JD-2440000	PHASE	FLUX MAGNITUDE		
LWR/LWP					(2150)	(2550)	(2950)
LWP 4088L	0:25	84/08/27.5	5939.964	0.29	6.38	6.45	6.51
LWP 4089H	13:	84/08/27.5	5939.995	0.29	6.23:	6.38:	6.38:
LWP 5252H	15:	85/01/23.2	6088.677	0.33	6.31:	6.38:	6.35:
LWP12533H	16:	88/01/20.2	7180.665	0.69	6.26:	6.54:	6.44:
SWP					(1450)	(1650)	(1850)
SWP23793L	0:50	84/08/27.5	5939.967	0.29	5.78	6.06	6.16
SWP24952L	0:50	85/01/23.2	6088.668	0.33	5.76	6.05	6.18
SWP32756L	0:45	88/01/20.2	7180.653	0.69	5.79	6.08	6.18

Si IV and C IV and definitive C II emission. Thus, we see an underlying B8–9 main-sequence spectrum with somewhat time-dependent signatures of heated gas. Although these three observations occurred near the two conjunction phases other spectra at similar phases do not show the enhancements, indicating an apparent lack of phase dependence.

5.3 *IUE Spectrophotometry*

Fluxes produced by the standard IUE calibrations have been corrected further for known instrumental effects: camera temperature dependencies and sensitivity degradation. The LWR sensitivity degradation correction for low-dispersion spectra (Clavel, Gilmozzi, and Prieto 1985) has been found by us to yield good results for

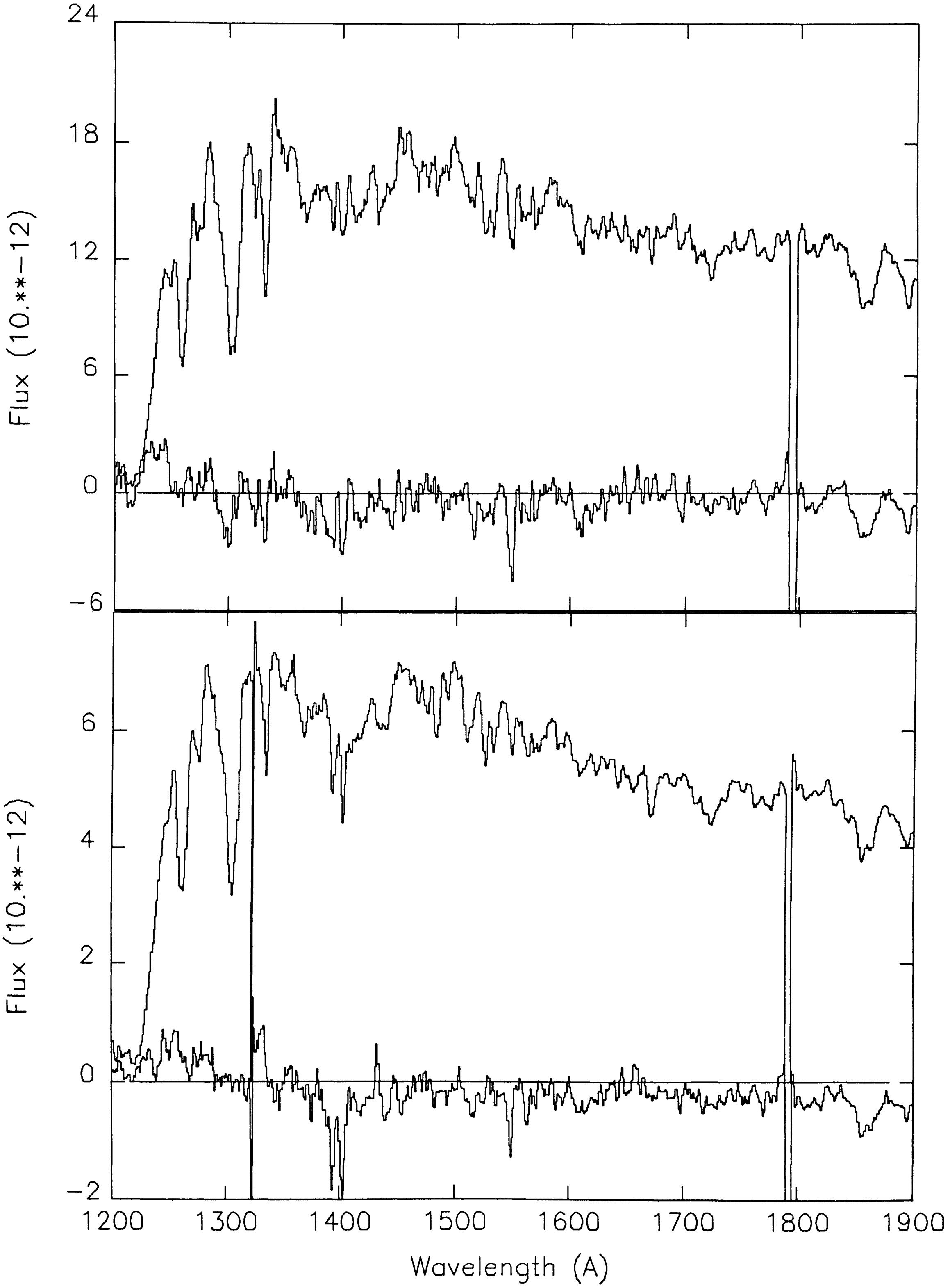

FIG. 7–Far-UV spectra of HD 43246 (top) and HD 127208 (bottom). Both may be classified as B8–9 III–Vp. The bottom of each panel displays the difference spectrum obtained by subtracting scaled fluxes of the B9 IV standard α Del. Important features are absorption at Si IV λ1394 and λ1403 and C IV λ1549 along with probable emission at C II λ1335. Spectra of HD 43246 exhibit variable Si IV, C IV, and C II features.

high-dispersion spectra as well. A test performed with high- and low-dispersion images of a nonvariable star taken on the same shift shows the fluxes to agree well when both are corrected with the same degradation function. Therefore, unlike standard IUE Regional Data Analysis Facility (RDAF) procedures, we also corrected the high-dispersion images (after compression to low resolution) with the Clavel *et al.* (1985) degradation function. The SWP data, which apparently suffer some degradation, have been corrected with a simple linear (in time) application of the Bohlin and Grillmaer (1988) preliminary results. The LWP images have been reprocessed with the corrected Intensity Transfer Function (Oliversen 1988).

The IUE fluxes are binned over 50 Å passbands centered at 1350 Å, 1450 Å, . . . 3150 Å. These data plus the ground-based Johnson system photometry are input to a composite energy distribution analysis program developed by Parsons (1981). This program plots, for comparison with the observations, energy distributions for specified combinations of two spectral types and V magnitudes plus interstellar extinction correction. By trial and error the program can produce very good fits for noninteracting binaries, and the resulting visual magnitude differences may be used to derive absolute magnitudes (Parsons and Ake 1987). The grid of intrinsic colors adopted by Parsons (1981) has been revised to include IUE flux information from standard stars.

Each epoch of HD 43246 and HD 127208 has been analyzed separately; sample fits to the energy distributions are shown in Figure 8. HD 43246 requires about an F8 primary, rather than the ground-estimated F2 spectral type, in order to fit the B magnitude; the primary is brighter than the hot secondary by about 1.0 magnitude in the V band. The *UBVRI* data for HD 127208 imply a mid-G-type star about 0.9 mag fainter in V than the B8–9 star. Neither binary system appears to be reddened by more than $E(B-V) = 0.04$.

The entire wavelength range cannot be fit with combinations of two normal energy distributions. The short wavelengths fit closely the B8 standard curve, but there is always excess flux of ~ 0.3 mag in the middle UV. Such excess flux could arise from the inner boundary region of an accretion disk (Bertout, Basri, and Bouvier 1988 and references therein). Alternatively, we can ignore the far-UV and fit the mid-UV region. This solution then requires hotter (by two subclasses) early type components, a rather large $E(B-V)$ (~ 0.16), and an unusual interstellar extinction law. Unfortunately, we then cannot match standard Lyman-α wings of the observed profiles with the appropriate hotter standard stars.

5.4 *IUE High-Resolution Spectroscopy*

Only mid-UV, not far-UV, high-dispersion observations were obtained for the systems under discussion. The main feature of interest in the mid-UV region is the Mg II resonance doublet (2795.5 Å, 2802.7 Å). Figure 9 shows samples of these resonance profiles at different epochs of HD 43246 and HD 127208, in comparison with the B9 IV standard spectrum.

Both binaries have strong circumstellar and/or interstellar absorption components near the rest wavelengths. For HD 43246, as in the Na D lines, this deep absorption appears stationary and occurs about $+10$ km s^{-1} from the γ velocity. The binaries also exhibit strong, broad emission components extending over several angstroms. The main difference between the Mg II profiles of the two systems is the terminal velocity (v_∞) of the strong wind absorption. For HD 43246 this velocity is normally about -140 km s^{-1} but is about -180 at two epochs. For HD 127208 the three epochs available give a range from -400 to -500 km s^{-1}.

For HD 43246 there are enough different epochs observed to see that the centroid of the Mg II emission varies in the same sense as the orbital motion of the *cool* component. Due to the overlying absorption, the centroid position is difficult to measure. The rough amplitude of the centroid motion is comparable to the orbital motion but displaced to more negative velocities.

6. Conclusions

The specific results of this research are summarized as follows:

(1) A new orbit has been calculated for HD 127208 and an improved one has been calculated for HD 43246.

(2) Analysis of photometry yielded estimates of stellar radii of the primary, the mean separation and sin i of the systems. The enlarged radii are larger than expected.

(3) Mass functions in conjunction with values for sin i indicate that the cooler, evolved stars in both binaries are the *less* massive components, implying that mass transfer has taken place in both systems.

(4) Double Na D lines and possibly the Mg II absorption indicate that mass loss from the systems, either due to winds from the components or Roche-lobe overflow, has produced a circumstellar shell.

(5) A mid-UV excess indicates the presence of additional luminous mass in the system, probably an accretion disk.

(6) For HD 127208 the primary source of the Hα emission appears to be the B star and is likely the result of mass transfer. Winds from both components are present. Similar, but less definite, results are found for HD 43246. A wind from either the B star or an accretion disk around the B star is present.

The research at the University of Toledo is supported by a grant from NASA (NAG5-254). With the support of NASA grants NAS 5-25774 and NAS 5-28749, S.B.P. obtained the IUE observations and performed their analysis at the Regional Data Analysis Facility of Goddard Space Flight Center.

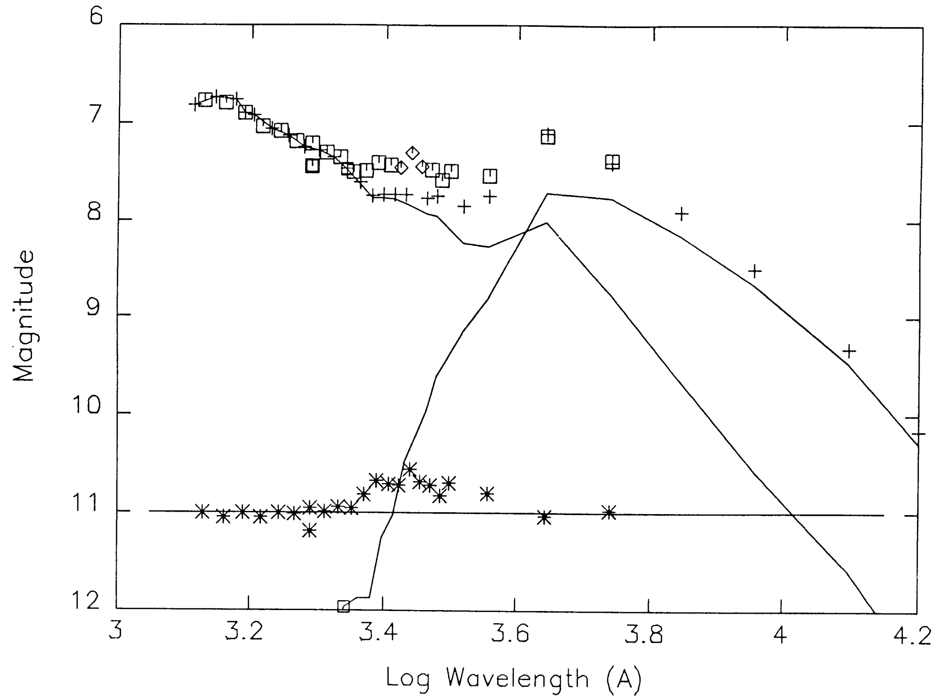

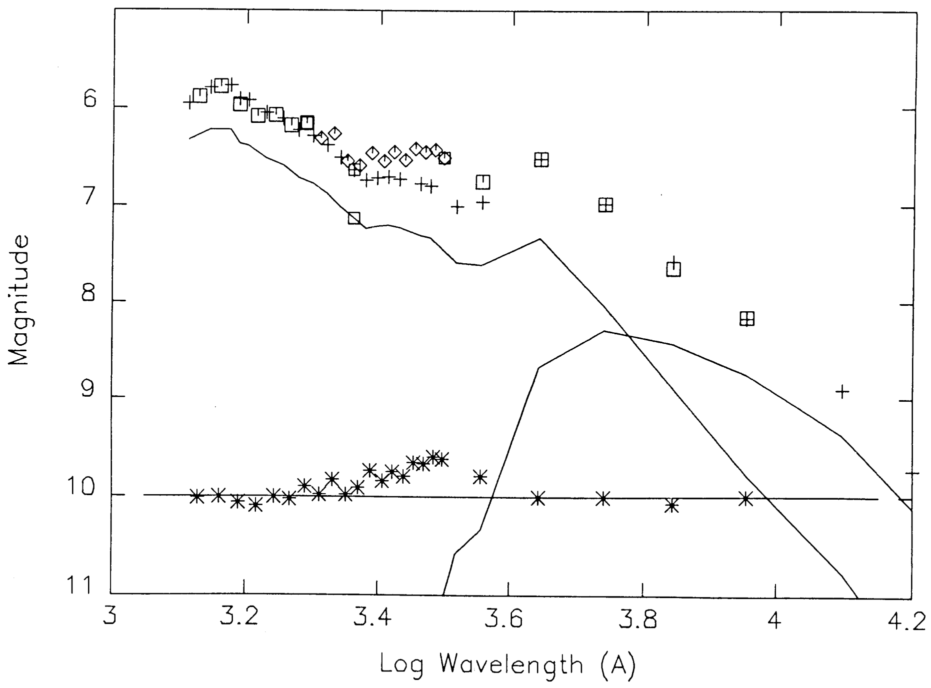

FIG. 8–Composite flux distributions of the systems and their analysis using standard-star energy distributions. Magnitudes on the same scale of energy as the *V* magnitude are plotted on a logarithmic wavelength scale. Squares and diamonds (for lower-weight data) represent the observed IUE and Johnson-system *UBVRI* data. Plus signs (+) show the best-fitting composite distributions from trial and error, while solid curves show the individual components to the fit. For HD 127208 only the B8 part of the average of B8 and B9 intrinsic colors is plotted as a solid curve. Along the bottom panel are plotted the $O-C$ differences. The parameters for the fits are:

Star	Spectral Types	ΔV	$E(B-V)$
HD 43246	F8 III + B8 V	+1.0	0.00
HD 127208	G6: III + B8.5 V	−0.9	0.04 .

The entire wavelength range cannot be fitted with combinations of two normal energy distributions; there is excess flux of about 0.3 mag in the mid-UV at all observed epochs. Such excess flux is believed to come from the inner boundary region of an accretion disk. The luminosity classes are taken from ground-based estimates.

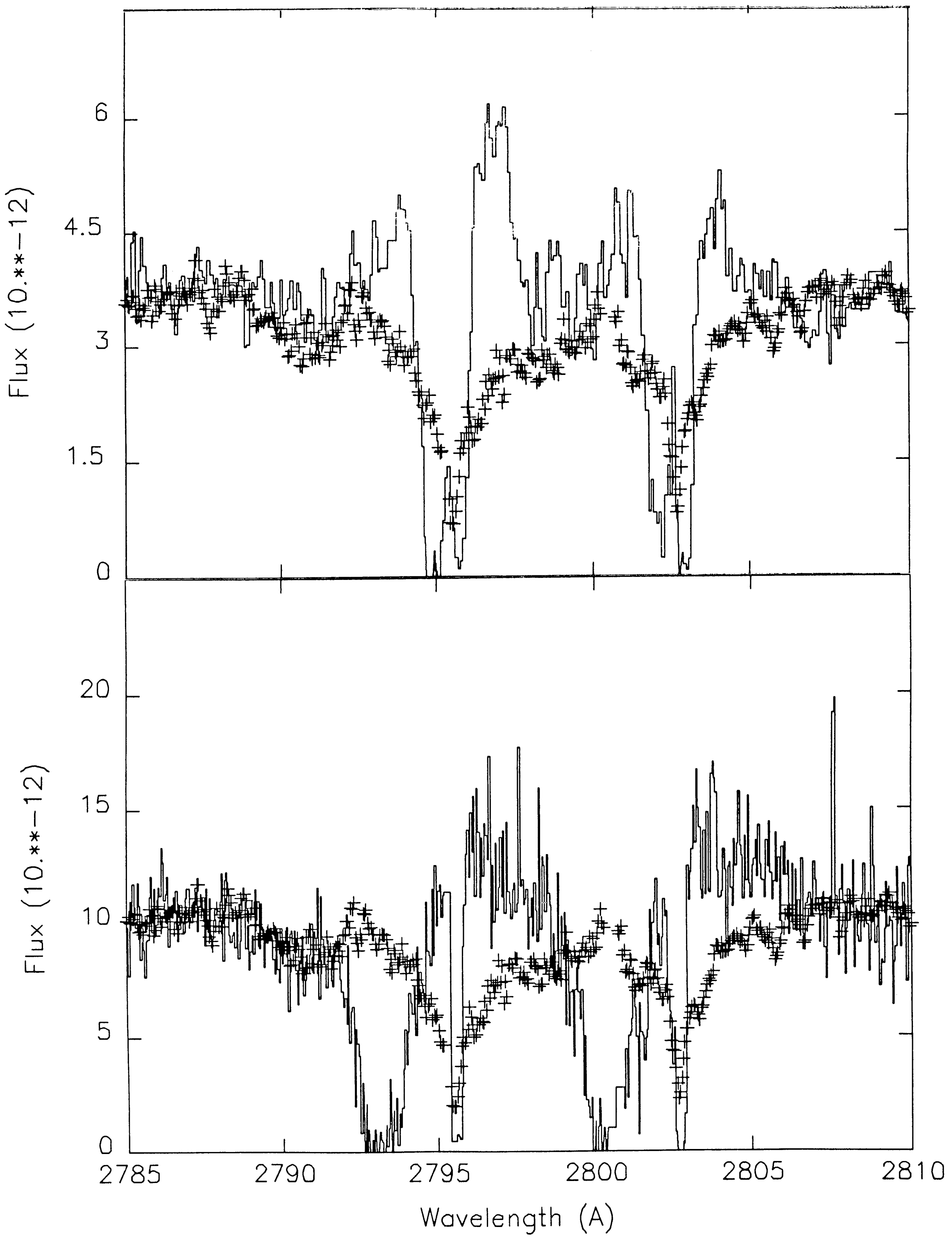

FIG. 9–High-dispersion IUE flux spectra of HD 43246 (top) and HD 127208 (solid curves) in the vicinity of the Mg II λλ2796,2803 resonance doublet. For comparison, plus signs (+) show the scaled spectrum of α Del. Both binaries have strong circumstellar and/or interstellar absorption components near the rest wavelengths. They also exhibit strong, broad emission components extending over several angstroms. The main difference between the profiles of the two systems is the terminal velocity of the strong wind absorption. For HD 43246 this velocity is normally about -140 km s^{-1} but it is about -180 at two epochs. For HD 127208, the three epochs available give a range from -400 to -500 km s^{-1}.

REFERENCES

Abt, H. A. 1983, *Ann. Rev. Astr. Ap.*, **21**, 343.

Abt, H. A., and Cardona, O. 1984, *Ap. J.*, **285**, 190.

Abt, H. A., and Levy, S. G. 1978, *Ap. J. Suppl.*, **36**, 241.

Allen, C. W. 1976, *Astrophysical Quantities* (3rd ed.; London: Athlone Press).

Barker, E. S., Evans, D. S., and Laing, J. D. 1967, *Roy. Obs. Bull.*, No. 130.

Batten, A. H. 1973, *Binary and Multiple Systems of Stars* (Oxford: Pergamon Press), p. 60.

Batten, A. H., Fletcher, J. M., and Mann, P. J. 1978, *Pub. Dom. Ap. Obs.*, **15**, 121.

Bertout, C., Basri, G., and Bouvier, J. 1988, *Ap. J.*, **330**, 350.

Bidelman, W. P. 1954, *Ap. J. Suppl.*, **1**, 175.

Bohlin, R. C., and Grillmaer, C. J. 1988, *Ap. J. Suppl.*, **66**, 209.

Bopp, B. W., and Meredith, R. 1986, *Pub. A.S.P.*, **98**, 772.

Bopp, B. W., Goodrich, B. D., Africano, J. L., Noah, P. V., Meredith, R. J., Palmer, L. H., and Quigley, R. J. 1984, *Ap. J.*, **285**, 202.

Bopp, B. W., Noah, P. V., and Jones, R. 1985, *Bull. AAS*, **17**, 574.

Burki, G., and Mayor, M. 1983, *Astr. Ap.*, **124**, 256.

Christie, W. H., and Wilson, O. C. 1938, *Ap. J.*, **88**, 34.

Clavel, J., Gilmozzi, R., and Prieto, A. 1985, *IUE NASA Newsletter*, No. 27, p. 50.

Dempsey, R., Parsons, S., and Bopp, B. W. 1988, *Pub. A.S.P.*, **100**, 581.

Fekel, F. C. 1988, *A.J.*, **95**, 215.

Fekel, F. C., Bopp, B. W., and Lacy, C. H. 1978, *A.J.*, **83**, 1445.

Gieren, W. 1982, *Ap. J. Suppl.*, **49**, 1.

Griffin, R. F., Parsons, S. B., Dempsey, R. C., and Bopp, B. W. 1990, *Pub. A.S.P.*, submitted.

Grygar, J., Cooper, M., and Jurkevich, I. 1972, *Bull. Astr. Inst. Czechoslovakia*, **23**, 147.

Hanuschik, R. W. 1986, *Astr. Ap.*, **166**, 185.

Kriz, S., and Harmanec, P. 1975, *Bull. Astr. Inst. Czechoslovakia*, **26**, 65.

Lloyd Evans, T. 1968, *M.N.R.A.S.*, **141**, 109.

Madore, B. F. 1977, *M.N.R.A.S.*, **178**, 505.

Madore, B. F., and Fernie, J. D. 1980, *Pub. A.S.P.*, **92**, 315.

Mayor, M., and Mazeh, T. 1987, *Astr. Ap.*, **171**, 157.

Merrill, P. W. 1942, *Pub. A.S.P.*, **54**, 155.

Morris, S. L. 1985, *Ap. J.*, **295**, 143.

Oliversen, N. A. 1988, *IUE NASA Newsletter*, No. 35, p. 55.

Pacynski, B. 1971, *Ann. Rev. Astr. Ap.*, **9**, 183.

Parsons, S. B. 1981, *Ap. J.*, **247**, 560.

Parsons, S. B., and Ake, T. B. 1987, *Bull. AAS*, **19**, 708.

Parsons, S. B., and Bopp, B. W., 1986, *Bull. AAS*, **18**, 682.

Peters, G. 1981, in *IAU Symposium 98, Be Stars*, ed. M. Jaschek and H. Groth (Dordrecht: Reidel), p. 311.

Petrie, R. M. 1948, *J.R.A.S. Canada*, **42**, 140.

Russo, G. 1982, in *Binary and Multiple Stars as Tracers of Stellar Evolution*, ed. Z. Kopal and J. Rahe (Dordrecht: Reidel), p. 23.

Slettebak, A. 1976, in *IAU Symposium 70, Be and Shell Stars*, ed. A. Slettebak (Dordrecht: Reidel), p. 123.

Underhill, A. 1982, in *B Stars With and Without Emission Lines*, ed. A. Underhill and V. Doazan (NASA SP-456).

Willmarth, D., and Abt, H. 1985, in *IAU Colloquium 88, Stellar Radial Velocities*, ed. A. G. D. Philip and D. W. Latham (Schenectady: L. Davis Press), p. 99.

Wolf, R. H., Horak, H. G., and Storer, N. W. 1967, in *Modern Astrophysics*, ed. M. Hack (New York: Gordon & Breach), p. 251.

Wu, C.C., *et al.*, 1983, *IUE NASA Newsletter*, No. 22, p. 1.